European Review for Medical and Pharmacological Sciences 2019; 23: 9566-9573

MicroRNA-577 inhibits cardiomyocyte apoptosis induced by myocardial infarction *via* targeting PARP1

Y.-H. WANG, X.-Y. ZHANG, Y.-Q. HAN, F. YAN, R. WU

Department of Cardio-Pulmonary Function, Fuwai Central China Cardiovascular Hospital (Henan Provincial People's Hospital Heart Centre), Zhengzhou, China

Abstract. – OBJECTIVE: The aim of this study was to investigate whether microRNA-577 could inhibit myocardial infarction (MI)-induced cardiomyocyte apoptosis by regulating poly ADP-ribose polymerase 1 (PARP1).

MATERIALS AND METHODS: MI model was successfully established in mice by ligation of the left anterior descending coronary artery (LAD). The expression levels of microRNA-577 and PARP1 in myocardial tissues of mice were examined by quantitative Real Time-Polymerase Chain Reaction (qRT-PCR). MI model in cells was established by hypoxia pre-treatment in primary cardiomyocytes and MCM cells. Subsequently, the expression levels of microRNA-577 and PARP1 in hypoxia preconditioning cardiomyocytes were determined as well. Meanwhile, Caspase3 activity in cardiomyocytes overexpressing microRNA-577 or PARP1 was detected using a relative commercial kit. Furthermore, the binding relationship between microRNA-577 and PARP1 was examined by Dual-Luciferase reporter gene assay.

RESULTS: Infarct size/risk region and risk region/LV in MI group were (62.1±2.2)% and (57.6±1.9)%, respectively. Both of the above two indexes in the MI group were significantly higher than those of the control group. The serum level of LDH in MI mice increased by 2.8-fold when compared with controls. Meanwhile, the expressions of microRNA-577 and PARP1 in myocardial tissues of MI mice were markedly down-regulated in a time-dependent manner. Compared with normoxia preconditioning cardiomyocytes, microRNA-577 expression in hypoxia preconditioning MCM cells and primary cardiomyocytes was remarkably decreased. Dual-Luciferase reporter gene assay confirmed that microRNA-577 could bind to PARP1. After transfection of microRNA-577 mimics, the expression of PARP1 was significantly down-regulated. Moreover, microRNA-577 over-expression inhibited caspase3 expression in hypoxia preconditioning cells, which could be reversed by PARP1 up-regulation. Similarly, microRNA-577 over-expression markedly decreased infarct size, risk region and serum level of LDH in MI mice, which could be reversed by PAPR1 over-expression.

CONCLUSIONS: MicroRNA-577 inhibits MI-induced cardiomyocyte apoptosis by degrading PARP1.

Key Words:
Myocardial infarction (MI), MicroRNA-577, Apoptosis.

Introduction

Myocardial infarction (MI) is a serious ischemic heart disease worldwide. MI is mainly caused by myocardial necrosis due to acute and persistent ischemia and hypoxia in coronary arteries[1]. Recent statistics have indicated that MI is one of the main factors that endanger human health and even causes cardiac death. Myocardial ischemia and hypoxia during MI can cause irreversible death or cell apoptosis, further leading to cardiac insufficiency[2]. Cardiomyocyte apoptosis exerts a vital role in cardiac remodeling and even heart failure after MI. Therefore, preventing cardiomyocyte apoptosis improves MI-induced cardiac dysfunction and cardiac remodeling process[3]. In recent years, studies have focused on searching for highly sensitive and specific hallmarks for diagnosis, prevention and control of MI[4,5].

MicroRNA (miRNA) participates in the development and progression of various diseases by inhibiting mRNA transcription or degradation[6]. Scholars[7,8] have shown that abnormal expression of miRNAs is closely related to the pathophysiological processes of multiple cardiovascu-

Corresponding Author: Rui Wu, MM; e-mail: 13513803991@163.com

lar diseases. Therefore, miRNA is believed to serve as diagnostic and prognostic biomarkers for diseases. Reserachers[9,10] have demonstrated that miRNA-208 is highly expressed in impaired myocardial tissues with high tissue-specificity. Moreover, Liang et al[11] have shown that miR-21 regulates cardiac fibrosis by targeting the expression of transforming growth factor (TGF) β III, thus mediating the progression of cardiac diseases.

Our previous results have found that microRNA-577 is lowly expressed in myocardial tissues of MI mice. However, the exact role of microRNA-577 in myocardial infarction has not been fully elucidated. The aim of this work was to investigate the role of microRNA-577 in MI and the possible underlying mechanism.

Materials and Methods

Establishment of the MI Model in Mice

C57BL/6 mice were first anesthetized by intraperitoneal injection of 0.8% chloral hydrate (50 mg/kg). The mice were then fixed at a supine position, and a longitudinal incision was made for heart exposure. Subsequently, muscles and tissues around the heart were bluntly separated. The left anterior descending coronary artery (LAD) ligation was performed using 7.0-suture. Pale left ventricular wall and decreased ventricular wall motion indicated the successful establishment of the MI model in mice. Meanwhile, mice in the control group were cut open without LAD ligation. This study was approved by the Animal Ethics Committee of the Henan Provincial People's Hospital Animal Center.

Evaluation of the MI Model in Mice

24 hours after animal procedures, mice were anesthetized for thoracotomy. Intracardiac injection of 0.5 mL 2% Evans blue was performed. Myocardial tissue in the non-ischemic area was stained blue, while the unstained part was the area at risk (AAR). Left ventricle (LV) was harvested and ice-cold for 30 min. Subsequently, tissues were sliced into 1-mm sections parallel to atrioventricular groove. After washing with Phosphate-Buffered Saline (PBS) three times, the sections were fixed in 10% paraformaldehyde, followed by capture under a microscope. Ischemic risk zone (including the infarct zone and the infarct border zone) was unstained by Evans Blue. However, the infarct border zone was stained red with 2,3,5-Triphenyte-trazolium-chloride (TTC). The infarct area was pale. The infarct size was calculated using the Osiris/Image ProPlus (Media Cybernetics, Silver Springs, MD, USA) as the ratio of infarct size and AAR. Serum samples were collected from each mouse, and the relative level of LDH was determined.

Cell Culture

Primary cardiomyocytes were extracted as previously described[12]. Primary cardiomyocytes were cultured in Dulbecco's Modified Eagle's Medium (DMEM; Gibco, Grand Island, NY, USA) containing 10% fetal bovine serum (FBS; Gibco, Grand Island, NY, USA), and maintained in a 5% CO_2 incubator at 37°C. During the first three days of culture, 0.1 mM BrdU was added in cells to inhibit the growth of non-cardiomyocytes. MCM cells were inoculated into DMEM containing 10% FBS with routine culture.

Hypoxia Preconditioning

Primary cardiomyocytes and MCM cells in logarithmic growth phase were randomly assigned to the four following groups: (1) Control group: normoxia preconditioning under 20% O_2; (2) Hypoxia 3 h group: hypoxia preconditioning under 0% O_2 for 3 h; (3) Hypoxia 6 h group: hypoxia preconditioning under 0% O_2 for 6 h; (4) Hypoxia 12 h group: hypoxia preconditioning under 0% O_2 for 12 h.

Cell Transfection

When the density of cells reached 50%, the cells were transfected with microRNA-577 mimics, pcDNA-PARP1 (poly ADP-ribose polymerase 1) or negative control according to the instructions of Lipofectamine 2000 (Invitrogen, Carlsbad, CA, USA). The fresh medium was replaced at 4-6 h after incubation. Quantitative Real Time-Polymerase Chain Reaction (qRT-PCR) was performed to verify transfection efficacy at 48 h.

RNA Extraction

Tissues (50 mg) or cells (5×10^6) were lysed in 1 mL of TRIzol (Invitrogen, Carlsbad, CA, USA) for 5 min of incubation. Subsequently, 200 μL of chloroform was added, mixed and stand at room temperature for 5 min. After centrifugation at 4°C, 12000 r/s for 15 min, the supernatant was transferred into a new RNase-free centrifuge tube. Isopropanol with an equal volume of the supernatant was added, followed by the harvest

of RNA precipitate by centrifugation. Extracted RNA was air dried, quantified and dissolved in 15-50 μL of diethyl pyrocarbonate (DEPC) water (Beyotime, Shanghai, China) for subsequent use.

Quantitative Real Time-Polymerase Chain Reaction

Extracted total RNA was reverse transcribed into complementary deoxyribose nucleic acid (cDNA) according to the instructions of PrimeScript RT reagent Kit (TaKaRa, Otsu, Shiga, Japan. Quantitative Real Time-Polymerase Chain Reaction (qRT-PCR) was carried out in accordance with SYBR Green PCR Kit (Applied Biosystems, Foster City, CA, USA). The total qRT-PCR system was 10 μL, and the specific procedure was as follows: pre-denaturation at 95°C for 2 min, followed by 40 cycles of denaturation at 95°C for 1 min, annealing at 60°C for 1 min and extension at 72°C for 1 min. Primer sequences used in this study were as follows: MicroRNA-577, F: 5'-ACACTCCAGCTGGGTAGATAAAATATTGG-3', R: 5'-CTCAACTGGTGTCGTGGAGTCGGCAATTCAGTTGAGCCATGGAC-3'; U6, F: 5'-CTCGCTTCGGCAGCACATATA-3', R: 5'-AAATATGGAACGCTTCACGA-3'; PARP1, F: 5'-GGAAAGGGATCTACTTTGCCG-3', R: 5'-TCGGGTCTCCCTGAGATGTG-3'; glyceraldehyde 3-phosphate dehydrogenase (GAPDH), F: 5'-GAAGAGAGAGACCCTCACGCTG-3', R: 5'-ACTGTGAGGAGGGGAGATTCAGT-3'.

Dual-Luciferase Reporter Gene Assay

The transcript 3'Untranslated Region (3'UTR) sequence of PARP1 was cloned into vector pGL3 containing Luciferase reporter gene, namely Wt PARP1 3'UTR group. Mut PARP1 3'UTR group was constructed by mutating core binding sequences using a site-directed mutagenesis kit (Thermo Fisher Scientific, Waltham, MA, USA). After that, the cells were co-transfected with microRNA-577 mimics/negative control and Wt PARP1 3'UTR/Mut PARP1 3'UTR, respectively. 24 hours after transfection, the cells were lysed and centrifuged at 10,000 g for 5 min. Finally, 100 μL of the supernatant was collected for Luciferase activity determination.

Cell Apoptosis

Cells were first washed twice with 1×Phosphate-Buffered Saline (PBS), digested with 0.25% trypsin and centrifuged at 2,000 rpm for 10 min at 4°C. The supernatant was removed, and the cell precipitation was stained according to the instructions of fluorescein isothiocyanate (FITC)/Annexin V apoptosis detection kit (BD Pharmingen, San Diego, CA, USA). Briefly, 500 μL of 1×buffer was added for cell resuspension. Then, 5 μL of Annexin V and Propidium Iodide (PI) were added to stain the cells at 37°C in the dark for 20 min. Finally, apoptosis of each sample was detected using flow cytometry (BD Pharmingen, San Diego, CA, USA).

Western Blot

Total protein in cells or tissues was extracted using radioimmunoprecipitation assay (RIPA; Beyotime, Shanghai, China). Extracted protein samples were separated by electrophoresis and transferred to polyvinylidene difluoride (PVDF) membranes (Millipore, Billerica, MA, USA) at 300 mA for 100 minutes. After blocking with 5% skimmed milk for 2 hours, the membranes were incubated with primary antibodies at 4°C overnight. On the next day, the membranes were incubated with secondary antibodies at room temperature for 2 hours. Bands were finally exposed by enhanced chemiluminescence (ECL) and analyzed by Image Software (NIH, Bethesda, MD, USA).

Caspase3 Activity Determination

Caspase3 activity was determined according to the instructions of the caspase colorimetric assay kit (KeyGEN, Nanjing, China). Briefly, 50 μL of PBS containing 150 g protein sample was applied to each well of 24-well plates. The protein sample was then incubated with isodose 2 × reaction buffer and caspase3 substrate at 37°C for 4 h in the dark. The control sample was 50 μL of PBS without proteins. The absorbance at the wavelength of 405 nm was determined. Caspase3 activity was calculated as the ratio of $A405_{sample}/A405_{control}$.

Statistical Analysis

Statistical Product and Service Solutions (SPSS) 18.0 (SPSS Inc., Chicago, IL, USA) was used for all statistical analysis. Data were represented as mean ± SD (standard deviation). The *t*-test was used to compare the differences between the two groups. One-way analysis of variance (ANOVA) was applied to compare the differences among different groups, followed by post-hoc test (Least Significant Difference). $p<0.05$ was considered statistically significant.

Results

MicroRNA-577 Was Lowly Expressed in the MI Model

24 h after LAD, we first examined the infarct size/risk region, risk region/left ventricle (LV) and serum level of LDH in mice. The data revealed that the infarct size/risk region in MI mice (62.1±2.2%) was significantly higher than that of controls at 24 h of LAD (Figure 1A). The risk region/LV in MI mice (57.6±1.9%) was markedly higher when compared with mice in the control group (Figure 1B). In addition, the serum level of LDH was remarkably higher in MI mice than controls (Figure 1C). The above data all confirmed successful construction of MI model in mice. To investigate whether microRNA-577 expression was influenced by MI, we detected the expression level of microRNA-577 in mouse myocardium at different time points. The results showed that microRNA-577 expression was significantly reduced in the myocardium of MI mice in a time-dependent manner (Figure 1D). Subsequently, *in vitro* MI model was established by hypoxia preconditioning in primary cardiomyocytes from MI mice and MCM cells. Identically, microRNA-577 expression in primary cardiomyocytes and MCM cells was gradually down-regulated under hypoxic condition (Figure 1E, 1F).

PARP1 Was the Target Gene of MicroRNA-577

Through online prediction and analysis, we found that PARP1 was a potential target gene for microRNA-577 (Figure 2A). MicroRNA-577 mimics was constructed and transfected into cells. The subsequent results indicated that microRNA-577 mimics transfection could markedly up-regulate microRNA-577 expression in MCM cells (Figure 2B). Furthermore, the Dual-Luciferase reporter gene assay confirmed the binding relationship of PAPR1 to microRNA-577 (Figure 2C). PARP1 expression in the *in vitro* MI model was time-dependently increased (Figure 2D). Both the mRNA and protein levels of PARP1 were significantly down-regulated after transfection of microRNA-577 mimics (Figure 2E). The above re-

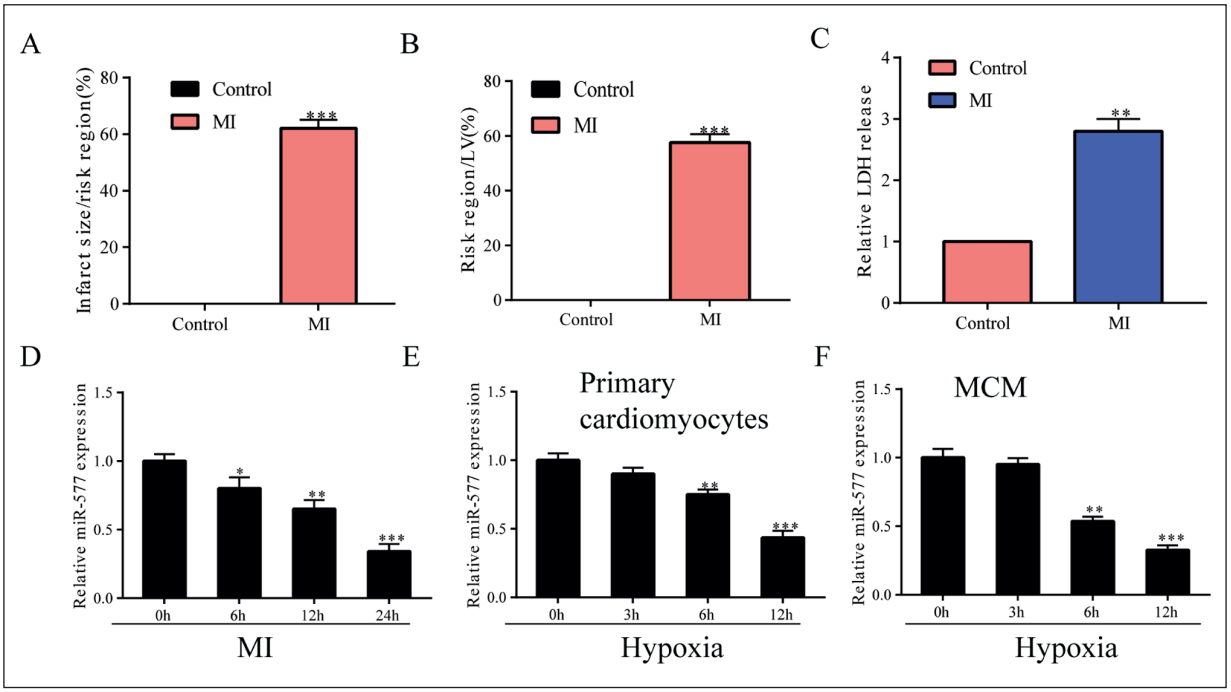

Figure 1. MiR-577 was lowly expressed in MI model. **A,** Infarct size/risk region (%) in mice of the control group and MI group at 24 h of LAD. **B,** Risk region/LV (%) in mice of the control group and MI group at 24 h of LAD. **C,** The relative LDH release in mice of control group and MI group at 24 h of LAD. **D,** The relative level of miR-577 in mouse myocardium of control group and MI group at 24 h of LAD. **E,** The relative level of miR-577 in primary cardiomyocytes under hypoxia condition for 0, 3, 6 and 12 h, respectively. **F,** The relative level of miR-577 in MCM cells under hypoxia condition for 0, 3, 6, and 12 h, respectively. *p<0.05, **p<0.01, ***p<0.001.

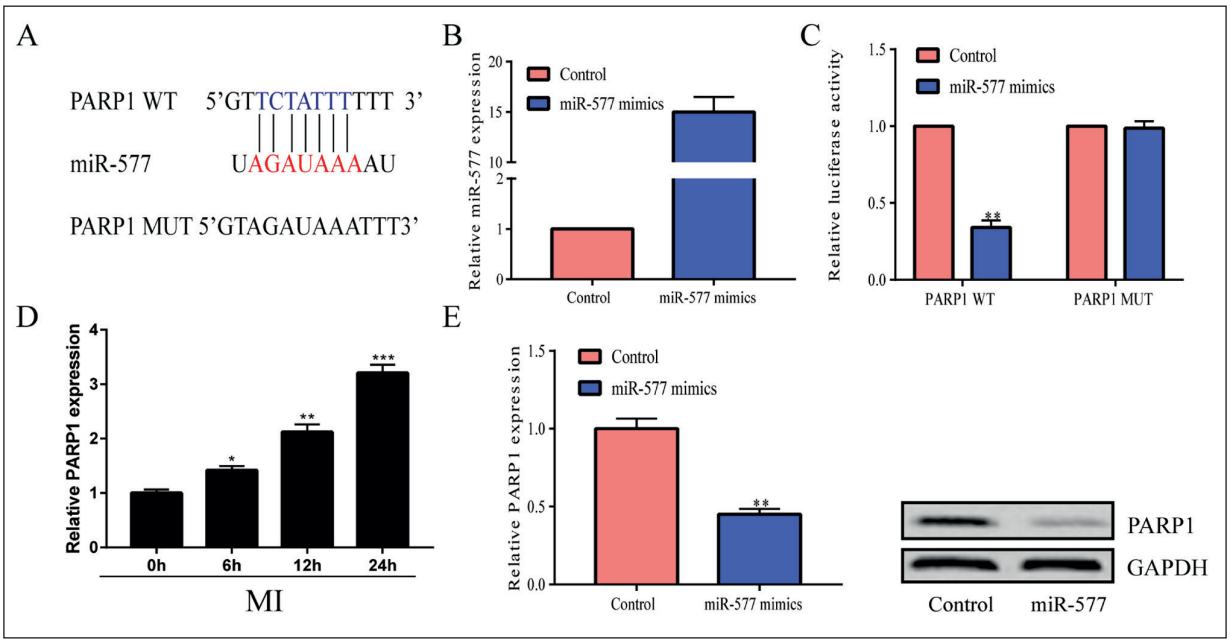

Figure 2. PARP1 was the target gene of miR-577. **A,** Potential binding sites between PAPR1 and miR-577. **B,** Transfection efficacy of miR-577 mimics in MCM cells. **C,** Dual-Luciferase reporter gene assay indicated the binding relationship between PAPR1 and miR-577. **D,** The relative level of PARP1 in MCM cells under hypoxia condition for 0, 6, 12, and 24 h, respectively. **E,** Transfection of miR-577 mimics in MCM cells significantly down-regulated PARP1 expression at both mRNA and protein levels. *p<0.05, **p<0.01, ***p<0.001.

sults indicated that PARP1 was the target gene and could be negatively regulated by microRNA-577.

MicroRNA-577 Inhibited AMI-Induced Cardiomyocyte Apoptosis

To explore the possible role of microRNA-577 in myocardial infarction, we constructed an *in vitro* MI model by hypoxia pre-treatment in MCM cells. QRT-PCR results demonstrated that Caspase3 expression in hypoxia preconditioning MCM cells was markedly higher than that of normoxia preconditioning cells. This indicated the successful construction of MI model *in vitro* (Figure 3A). Under hypoxia condition, MCM cells over-expressing PARP1 showed significantly elevated caspase3 activity (Figure 3B). On the contrary, microRNA-577 over-expression remarkably inhibited caspase3 activity in hypoxia preconditioning MCM cells, suggesting inhibited apoptosis of cardiomyocytes (Figure 3C). Subsequently, we evaluated the role of microRNA-577 in the MI model *in vivo*. The data revealed that microRNA-577 over-expression markedly reduced risk region/LV, infarct size/risk region and serum level of LDH in MI mice when compared with controls (Figure 3D-3F).

MicroRNA-577 Inhibited AMI-Induced Cardiomyocyte Apoptosis via Targeting PARP1

To explore whether microRNA-577 exerted its role in MI by targeting PARP1, we co-overexpressed microRNA-577 and PARP1 in cardiomyocytes. Caspase3 expression in hypoxia preconditioning MCM cells co-overexpressing microRNA-577 and PARP1 was significantly higher than those overexpressing miR-377 (Figure 4A). Similar results were obtained in the *in vivo* MI model as well. Co-overexpression of microRNA-577 and PARP1 could reverse the inhibitory effects of microRNA-577 on risk region/LV, infarct size/risk region and serum level of LDH in AMI mice (Figure 4B-4D). All the results indicated that PARP1 partially reversed the inhibitory effect of microRNA-577 on cardiomyocyte apoptosis and its protective effect on MI.

Discussion

Apoptosis is a gene-regulated cell suicidal behavior with biochemical and morphological characteristics[13]. Inhibition of apoptosis results in abnormal proliferation instead of cell death, lead-

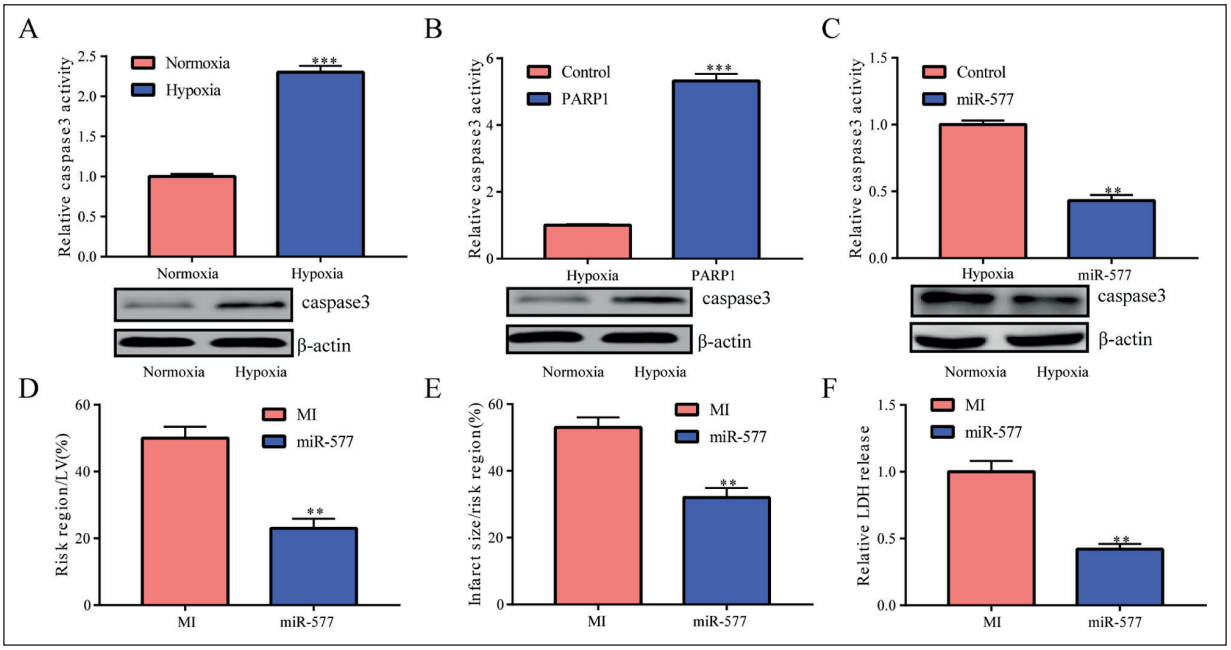

Figure 3. MiR-577 inhibited AMI-induced cardiomyocyte apoptosis. **A,** Caspase3 expression in MCM cells under normoxia or hypoxia condition. **B,** PAPR1 over-expression enhanced caspase3 expression in hypoxia preconditioning MCM cells. **C,** MiR-577 over-expression down-regulated caspase3 expression in hypoxia preconditioning MCM cells. **D,** Risk region/LV (%) decreased in MI mice over-expressing miR-577. **E,** Infarct size/risk region (%) decreased in MI mice over-expressing miR-577. **F,** The relative LDH release decreased in MI mice over-expressing miR-577. **p<0.01, ***p<0.001.

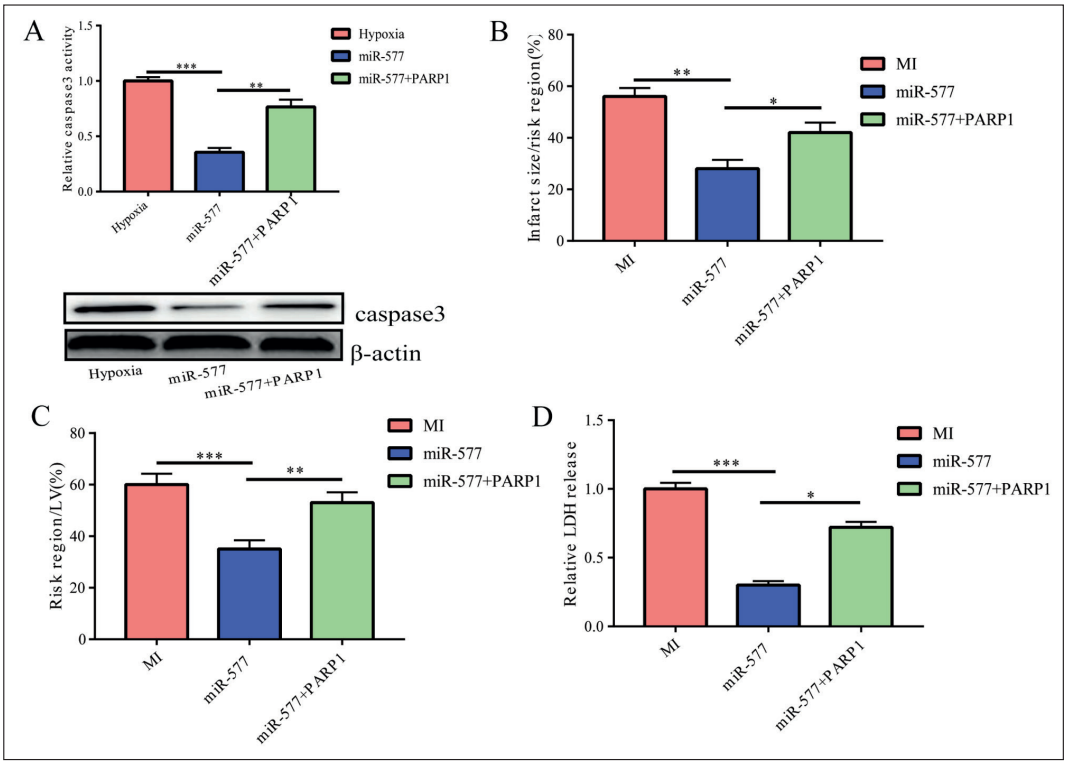

Figure 4. MiR-577 inhibited AMI-induced cardiomyocyte apoptosis *via* targeting PARP1. **A,** Expression of caspase3 in hypoxia preconditioning MCM cells co-overexpression miR-577 and PARP1 was significantly higher than those over-expressing miR-377. **B-D,** Co-overexpression of miR-577 and PARP1 reversed the inhibitory effects of miR-577 on risk region/LV; **B**, Infarct size/risk region; **C,** Serum level of LDH; **D,** In AMI mice. *p<0.05, **p<0.01, ***p<0.001.

ing to tumorigenesis and tumor development[14]. Cell proliferation and apoptosis are the basis for the body to maintain its own stability. Caspase, especially caspase3, plays a crucial role in the process of apoptosis[15]. A large number of cardiomyocyte apoptosis occur in the development of MI[16]. Therefore, the inhibition of cardiomyocyte apoptosis and minimization of cardiomyocyte damage have been well concerned in MI treatment. In this work, microRNA-577 was lowly expressed in myocardial tissues of MI mice and hypoxia preconditioning cardiomyocytes. Zhang et al[17] have shown that microRNA-577 suppresses tumor growth. Here, we aimed to explore the exact role of microRNA-577 in MI and its possible underlying mechanism. We found that microRNA-577 over-expression significantly inhibited caspase3 activity. This suggested the inhibitory effect of microRNA-577 on the apoptosis of MCM cells. Furthermore, microRNA-577 over-expression markedly decreased the infarct size, risk region and serum level of LDH in MI mice, exerting a protective role in AMI.

PARP1 (Poly (ADP-ribose) polymerase 1) locates on the q41-42 region of chromosome 1 (base positions of 224, 615, 015-224, 662, 424), with 47,410 bp in size. PAPR1 is mainly distributed in the promoter of encoded proteins, nucleoli and telomeres[18,19]. As a nuclear protein, PARP1 can be cleaved by activated caspase3 to form an apoptotic fragment. Several authors[20,21] have demonstrated that PARP1 is involved in the execution of apoptosis. In this work, bioinformatics predicted that PARP1 was a potential target gene of microRNA-577. Subsequent Dual-Luciferase reporter gene assay confirmed our hypothesis. PARP1 was highly expressed in myocardial tissues of MI mice and hypoxia preconditioning cardiomyocytes. The over-expression of PARP1 induced the release of caspase3, which further accelerated cardiomyocyte apoptosis. Hence, we speculated that microRNA-577 exerted its biological function in MI *via* targeting PARP1.

Subsequently, MCM cells were co-overexpressed with microRNA-577 and PARP1. MicroRNA-577 over-expression significantly decreased caspase3 activity, which could be partially reversed by co-overexpression of microRNA-577 and PARP1. This indicated that PAPR1 could partially reverse the inhibitory effect of microRNA-577 on MI-induced cardiomyocyte apoptosis. Similarly, PARP1 over-expression reversed the inhibitory effects of microRNA-577 on infarct size, risk region and serum level of LDH. All our findings suggested that the protective effect of microRNA-577 on MI relied on PARP1 degradation.

Conclusions

These results indicate that microRNA-577 inhibits MI-induced cardiomyocyte apoptosis by degrading PARP1, which can be utilized as a novel therapeutic target for MI.

Conflict of Interest

The Authors declare that they have no conflict of interests.

References

1) White HD, Thygesen K, Alpert JS, Jaffe AS. Clinical implications of the Third Universal Definition of Myocardial Infarction. Heart 2014; 100: 424-432.
2) Qiu H, Liu JY, Wei D, Li N, Yamoah EN, Hammock BD, Chiamvimonvat N. Cardiac-generated prostanoids mediate cardiac myocyte apoptosis after myocardial ischaemia. Cardiovasc Res 2012; 95: 336-345.
3) Abbate A, Narula J. Role of apoptosis in adverse ventricular remodeling. Heart Fail Clin 2012; 8: 79-86.
4) Goretti E, Wagner DR, Devaux Y. miRNAs as biomarkers of myocardial infarction: a step forward towards personalized medicine? Trends Mol Med 2014; 20: 716-725.
5) Fathil MF, Md AM, Gopinath SC, Hashim U, Adzhri R, Ayub RM, Ruslinda AR, Nuzaihan MNM, Azman AH, Zaki M, Tang TH. Diagnostics on acute myocardial infarction: cardiac troponin biomarkers. Biosens Bioelectron 2015; 70: 209-220.
6) Vogel B, Keller A, Frese KS, Kloos W, Kayvanpour E, Sedaghat-Hamedani F, Hassel S, Marquart S, Beier M, Giannitis E, Hardt S, Katus HA, Meder B. Refining diagnostic microRNA signatures by whole-miRNome kinetic analysis in acute myocardial infarction. Clin Chem 2013; 59: 410-418.
7) Harada M, Luo X, Murohara T, Yang B, Dobrev D, Nattel S. MicroRNA regulation and cardiac calcium signaling: role in cardiac disease and therapeutic potential. Circ Res 2014; 114: 689-705.
8) Yang QH, Yang M, Zhang LL, Xiao MC, Zhao Y, Yan DX. The mechanism of miR-23a in regulating myocardial cell apoptosis through targeting FoxO3. Eur Rev Med Pharmacol Sci 2017; 21: 5789-5797.
9) Satoh M, Minami Y, Takahashi Y, Tabuchi T, Nakamura M. Expression of microRNA-208 is associated with adverse clinical outcomes in human dilated cardiomyopathy. J Card Fail 2010; 16: 404-410.

10) Wojciechowska A, Braniewska A, Kozar-Kaminska K. MicroRNA in cardiovascular biology and disease. Adv Clin Exp Med 2017; 26: 865-874.

11) Liang H, Zhang C, Ban T, Liu Y, Mei L, Piao X, Zhao D, Lu Y, Chu W, Yang B. A novel reciprocal loop between microRNA-21 and TGFbetaRIII is involved in cardiac fibrosis. Int J Biochem Cell Biol 2012; 44: 2152-2160.

12) Nigro JM, Cho KR, Fearon ER, Kern SE, Ruppert JM, Oliner JD, Kinzler KW, Vogelstein B. Scrambled exons. Cell 1991; 64: 607-613.

13) Hengartner MO. The biochemistry of apoptosis. Nature 2000; 407: 770-776.

14) Reed JC. Dysregulation of apoptosis in cancer. Cancer J Sci Am 1998; 4 Suppl 1: S8-S14.

15) Tian X, Shi Y, Liu N, Yan Y, Li T, Hua P, Liu B. Upregulation of DAPK contributes to homocysteine-induced endothelial apoptosis via the modulation of Bcl2/Bax and activation of caspase 3. Mol Med Rep 2016; 14: 4173-4179.

16) Qu S, Yang X, Li X, Wang J, Gao Y, Shang R, Sun W, Dou K, Li H. Circular RNA: A new star of noncoding RNAs. Cancer Lett 2015; 365: 141-148.

17) Zhang W, Shen C, Li C, Yang G, Liu H, Chen X, Zhu D, Zou H, Zhen Y, Zhang D, Zhao S. miR-577 inhibits glioblastoma tumor growth via the Wnt signaling pathway. Mol Carcinog 2016; 55: 575-585.

18) Krishnakumar R, Gamble MJ, Frizzell KM, Berrocal JG, Kininis M, Kraus WL. Reciprocal binding of PARP-1 and histone H1 at promoters specifies transcriptional outcomes. Science 2008; 319: 819-821.

19) Salvati E, Scarsella M, Porru M, Rizzo A, Iachettini S, Tentori L, Graziani G, D'Incalci M, Stevens MF, Orlandi A, Passeri D, Gilson E, Zupi G, Leonetti C, Biroccio A. PARP1 is activated at telomeres upon G4 stabilization: possible target for telomere-based therapy. Oncogene 2010; 29: 6280-6293.

20) Villa P, Kaufmann SH, Earnshaw WC. Caspases and caspase inhibitors. Trends Biochem Sci 1997; 22: 388-393.

21) Kraus WL. Transcriptional control by PARP-1: chromatin modulation, enhancer-binding, coregulation, and insulation. Curr Opin Cell Biol 2008; 20: 294-302.